

Retrofitting reinforced concrete beams by bolting steel plates to their sides. Part 2: Transverse interaction and rigid plastic design

Deric John Oehlers[†], Marfique Ahmed[‡] and Ninh T. Nguyen^{††}

Department of Civil and Environmental Engineering, The University of Adelaide, SA 5005, Australia

Mark Andrew Bradford^{‡‡}

Department of Structural Engineering, University of New South Wales, NSW 2052, Australia

Abstract. In a companion paper, tests on bolted side plated beams have shown that side plates can substantially increase the strength of existing reinforced concrete beams with little if any loss of ductility and, furthermore, induce a gradual mode of failure after commencement of concrete crushing. However, it was also shown that transverse interaction between the side plates and the reinforced concrete beam, that is vertical slip and which is a concept unique to side plated beams, is detrimental. Transverse interaction increases the forces on the bolt shear connectors and, hence, weakens the beam. It also reduces the ability of the composite plated beam to yield and, hence, to attain its full flexural capacity. The generic concept of transverse interaction will be described in this paper and the results used to develop a new form of rigid plastic analysis for bolted side plated beams which is illustrated with an application.

Key words: retrofitting; rehabilitation; composite; reinforced concrete; plated beams; transverse interaction.

1. Introduction

Increasing the strength of existing reinforced concrete beams by bonding steel plates to their tension faces can be severely restricted by the loss of ductility associated with the increase in tension reinforcement. In contrast, tests have shown (Ahmed 1996, Ahmed, Oehlers and Bradford 2000) that bolting steel plates to the sides of reinforced concrete beams can substantially increase the strength, enhance the ductility and induce a gradual mode of failure. However, these tests have also shown that the transverse action between the plates and the reinforced concrete beam imposes additional shear forces at the plate/beam interface. Furthermore, the transverse action reduces the curvature in the plate and, hence, its ability to yield. Both of these transverse partial interaction effects need to be allowed for in design.

The tests reported in the companion paper (Ahmed, Oehlers and Bradford 2000) showed that a

[†] Senior Lecturer

[‡] Former Postgraduate Student

^{††} Former Research Fellow

^{‡‡} Professor

substantial portion of the plates remained elastic at failure and, hence, the bolted-side-plate analysis technique, that is developed in this paper, has to allow for partial yielding. To do this, two forms of analysis are used to determine the bounds that are used in the bolted-side-plate analysis. These analyses are: the side-plated rigid-plastic analysis technique developed in the companion paper where all three elements, that is the reinforced concrete beam, the plates and the bolt shear connectors, are assumed to be fully yielded or plastic; and a mixed-analysis approach (Oehlers and Sved 1995) where the bolt shear connection is assumed to be fully plastic but the plates and the reinforced-concrete beam are assumed to remain elastic.

The concept of transverse partial-interaction will first be illustrated by studying the distribution of the transverse slip using a mixed-analysis approach. The aim of this section is to give the reader an insight into the behaviour of this unique concept of transverse interaction. Bounds to the transverse forces and the moments these transverse forces induce in the plate elements are then developed using both the rigid-plastic and mixed analysis approaches. It is then shown how the rigid-plastic analysis technique for side plated beams, developed in the companion paper, can be adapted to incorporate these bounds to the transverse forces to form the bolted-side-plate analysis. This new bolted-side-plate analysis technique is then used to re-analyse the plated beam tests described in the companion paper in order to provide design rules that allow for the reduction in strength due to the neutral axis separation h_{na} and difference in curvature $\Delta\kappa$ effects, also described in the companion paper. The application of this new bolted-side-plate analysis technique is then illustrated. It must be emphasised that plate buckling (Smith, Bradford and Oehlers 1999a-b) and methods for preventing premature failure of the bolt-shear-connections (Ahmed 1996) are dealt with elsewhere.

2. Transverse slip

A mixed analysis will be used to gain an insight into the variation of the vertical slip. The beam in Fig. 1(a) is subjected to a point load of $2F$ at mid-span and the transverse forces in each shear span V are assumed to act at the ends of the shear span of length L_{ss} . The mixed analysis is illustrated in Fig. 2 where it is assumed that the plate and concrete elements remain linear-elastic, whereas, the bolt-shear-connectors are assumed to be fully plastic and, hence, the forces F_{RC} and F_p in Fig. 2(b) are equal to the strength of the shear connectors H in the shear span. Because of transverse partial interaction that is vertical slip, the curvature in the concrete element κ_{RC} in Fig. 2(c) is larger than that in the plate κ_p (Ahmed, Oehlers and Bradford 2000).

From equilibrium of the stress resultants at the cross-section in Fig. 2(b) which is situated at a distance x from the end of the shear span

$$M_{RC}(x) = M(x) - M_p(x) - H(x)h_{cnt} \quad (1)$$

where M =applied moment, M_p =moment in the plate, M_{RC} =moment in the concrete element, H =strength of shear connection over span x , and h_{cnt} =distance between the centroid of the steel elements and the centroid of the reinforced concrete element. From Fig. 1(a), the variation in the moment in the plate is $M_p(x) = Vx$ and the variation in the applied moment is $M(x) = Fx$ and, therefore, substituting these moments into Eq. (1) gives

$$M_{RC}(x) = Fx - Vx - qxh_{cnt} \quad (2)$$

where q =longitudinal shear flow strength across the plate/beam interface and which is assumed to

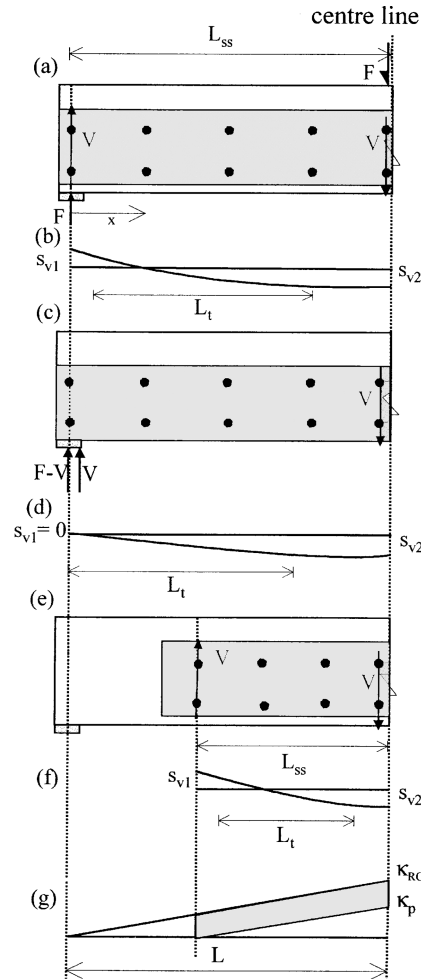


Fig. 1 Distribution of vertical slip

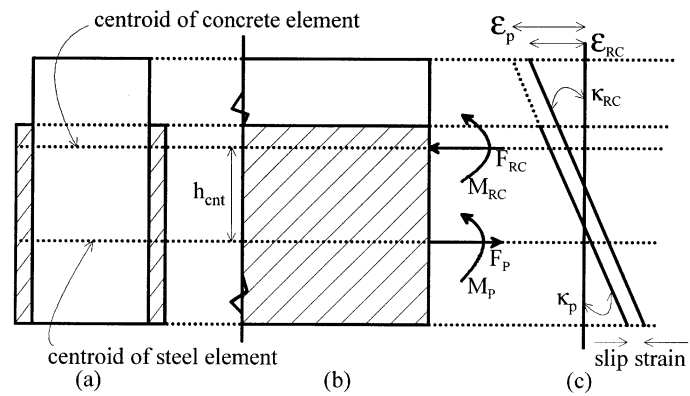


Fig. 2 Mixed analysis for longitudinal slip

be constant, that is, there is a uniform distribution of shear connectors. Substituting $M_{RC}(x) = (EI)_{RC} d^2y/dx^2$ where $(EI)_{RC}$ = flexural rigidity of the reinforced concrete element, and integrating twice, bearing in mind that the concrete element has zero slope at mid-span and zero deflection at the support, gives the following deflection of the reinforced concrete element at mid-span

$$y_{RC}(x = L_{ss}) = -\frac{(F - V - qh_{ent})L_{ss}^3}{3(EI)_{RC}} \quad (3)$$

A similar analysis can be applied to the plate element. In this case, the restraints applied to the plate ends can vary as will be shown subsequently, however, the change in the deflection of the plate between the support and the mid-span can be determined as

$$\Delta y_p = -\frac{VL_{ss}^3}{3(EI)_p} \quad (4)$$

where $(EI)_p$ = flexural rigidity of the plate elements. Eqs. (3) and (4) can be used to plot the shapes off the vertical slip distributions in Fig. 1 for various plate end restraints and positions.

Let us first consider the plated beam in Fig. 1(c) in which both the plate and the beam are resting on the support so that the vertical slip between the beam and the plate at the support $s_{v1} = 0$ as shown. In this case in which the plate is resting on the support, the slip at mid-span is given by Eq. (3) minus Eq. (4), which can be written as

$$[\Delta y_p]_{rest} = s_v - y_{RC}(x = L_{ss}) \quad (5)$$

where s_v is the slip required to achieve the transverse force V and where the plate slips upwards relative to the beam. When the plate is free of the support as shown in Fig. 1(a), then the plate above the supports must slip vertically downwards relative to the beam so that the bolt shear connectors achieve the force V which is in the opposite direction to that at mid-span. If we assume that $s_{v1} = s_{v2} = s_v$, as the transverse force V at mid-span is the same as that at the support, then the change in deflection of the plate over the shear span when the plate is free of the support is given by

$$[\Delta y_p]_{free} = 2s_v - y_{RC}(x = L_{ss}) \quad (6)$$

The change in the deflection required when the plate end is free of the support, $[\Delta y_p]_{free}$ in Eq. (6), is larger than that required when the plate is resting on the support, $[\Delta y_p]_{rest}$ in Eq. (5). To achieve this increase in deflection, the plate curvatures κ_p in the plated beam in Fig. 1(a) must be larger than those in the plated beam in Fig. 1(c). It was shown in the companion paper that it is difficult to achieve large curvatures in the plate and, hence, the beam with the plate that is free of the support in Fig. 1(a) is likely to be weaker than the beam in Fig. 1(c) in which the plate is resting on the support.

An alternative way of visualising the effect of the plate-end restraints is that the total relative slip in Fig. 1, which is $s_{vt} = |s_{v1}| + |s_{v2}|$, can be obtained by integrating twice the difference in the plate and concrete curvatures, $\Delta\kappa = \kappa_c - \kappa_p$, along the shear span. In which case, the beam in Fig. 1(a) would require a difference in curvature of at least twice that for the beam in Fig. 1(c). As the strength of the composite plated beam has been shown to reduce with increasing $\Delta\kappa$, the beam in Fig. 1(a), in which the plate is totally supported by the shear connectors, will be weaker than the beam in Fig. 1(c) in which the connectors transfer transverse shear forces only at mid-span. It can also be seen in Fig. 1(c) that the total transverse force resisted by the connectors is V that is the vertical force near mid-span, whereas it is $2V$ in Fig. 1(a). Hence, the connector shear strength

remaining to resist the longitudinal forces in the beam in Fig. 1(a) will be less than in the beam in Fig. 1(c) and, therefore, the beam in Fig. 1(a) will be even weaker than the beam in Fig. 1(c). The effect of terminating the plate short of the support as in Fig. 1(e) produces the slip distribution in Fig. 1(f) which can be obtained by integrating the difference in curvatures in Fig. 1(g). The shape of the slip distribution in Fig. 1(f) is the same as in Fig. 1(b) but the change in slip has to occur over a much shorter length of beam which will require a larger $\Delta\kappa$ which will further reduce the strength.

The distribution of vertical slip in Figs. 1(b), (d) and (f) also represents the distribution of transverse forces. In order to determine the magnitude of the transverse forces in the next section, it is necessary to quantify the distance between the resultant transverse forces L_t . From a study of both the theoretical vertical slip distributions such as that shown in Fig. 1 and the experimental vertical slip distributions (Ahmed 1996), it will be assumed for the bolted-side-plate analysis that the lever arm is given by

$$L_t = 0.7L_{ss} \quad (7)$$

where L_{ss} = length of the plate shear span as shown in Fig. 1.

3. Transverse forces

The stress resultants in a shear span of a plate element are shown in Fig. 3. It will be assumed that connectors either transfer the longitudinal forces H or they transfer the transverse forces V , so that the resultant force in a connector is either horizontal or vertical as shown in Fig. 3. It will be assumed that two groups of connectors transfer the transverse forces V and that these groups are spaced L_t apart. The remaining connectors transfer the longitudinal force H which in this case is shown to act at the mid-depth or centroid of the plate in Fig. 3. However, the force H can be eccentric to the centroid of the plate in which case, as will be shown in a later section, the eccentricity can easily be allowed for. The problem is to predict the moment in the plate at failure $M_{plate} = VL_t$ from which the transverse force V can be predicted.

As the load F in Fig. 1(a) is gradually applied to the composite plated beam, the plate goes through different stages: initially it will be elastic; it may then yield; and may then approach full plasticity. Failure of the composite plated beam, through crushing of the concrete in the reinforced concrete element, may occur at any of these stages of the plate element, which makes the problem of predicting the actual moment in the plate at the commencement of concrete failure extremely complex. So instead of trying to predict the actual moment in the plate at failure, the moment in the

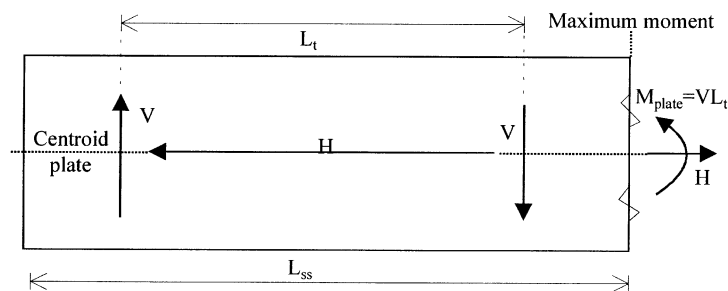


Fig. 3 Stress resultants in plate

plate at failure will be determined from the following two procedures: the mixed analysis for the condition when the plate is elastic $(M_{plate})_{mix}$; and the side-plate rigid plastic analysis for when the plate is fully plastic $(M_{plate})_{rpa}$. The larger of these two plate moments can then be used to derive an upper bound to the transverse forces V .

3.1. Rigid plastic analysis

A detailed description of a full-shear-connection full-interaction and a partial-shear-connection partial-interaction analysis are given in the companion paper. These analyses have been used to determine the variation of the moment capacity M_{comp} in Fig. 4(a) for the composite shallow plated beams B11 and B12 in the companion paper, for all degrees of shear connection η . It was assumed in the analysis (Ahmed and Oehlers 1997) that the neutral axis depth parameter $\gamma=1$. Denoting the longitudinal strength of the shear connection required for the full-shear-connection full-interaction analysis as $H_{fsc,fi}$ and the strength of the shear connection provided for the longitudinal forces as H so that the degree of shear connection can be defined as $\eta=H/H_{fsc,fi}$. Point A in Fig. 4(a) at $H=0$, that is at $\eta=0$, is the sum of the flexural strength of the reinforced concrete beam $M_{RC}=132$ kNm and the flexural strength of the steel plates acting independently $M_p=20$ kNm, therefore, $(M_{comp})_{\eta=0}=151$ kNm. Whereas, point B is the strength of the composite section with full-interaction and full-shear-connection which is $(M_{comp})_{\eta=1}=227$ kNm where $H=543$ kN.

The variation in strength from points A to B in Fig. 4(a) can be determined from the partial-shear-connection partial-interaction analysis described in the companion paper. This analysis can also be used to determine the variation in the moment in the plate $(M_{plate})_{rpa}$ as shown in Fig. 5. For example, for a given strength of shear connection H , the strain profiles in Fig. 5(b) are moved up and down independently of each other until each element is in equilibrium with the specified shear strength H , that is the resultant of the forces in Figs. 5(d) and (f) is equal to the strength of the shear connection H . The forces in the plate can now be visualised as a compressive component F_{cmp} at the top of the plate in Fig. 5(f) and a tensile component of equal magnitude at the bottom of the plate as shown, such that the remaining force in the plate is equal to the strength of the shear connection H . The moment in the plate M_{plate} is then quite simply the couple induced by the forces F_{cmp} . Hence, $(M_{plate})_{rpa}$ can be determined for any degree of shear connection as shown in Fig. 4(a). It can be seen that $(M_{plate})_{rpa}$ is at a maximum at $\eta=0$ where $(M_{plate})_{rpa}=20$ kNm, which is the flexural capacity of the plate and which is 9% of the full-shear-connection strength $(M_{comp})_{fsc}$. Furthermore, $(M_{plate})_{rpa}$ reduces to zero at $\eta=1$ where the plate is fully yielded in tension as the neutral axis lies above the plate in this specimen. It is worth noting that $(M_{plate})_{rpa} > 0$ for all beams with partial-shear-connection.

As can be seen in Fig. 3, the transverse shear force V is given by M_{plate}/L_t . Furthermore from Fig. 3, each shear span requires connectors of strength $2V$. The variation in the transverse shear connector strength required to induce M_{plate} is plotted in Fig. 4(b) in terms of the longitudinal strength of shear connection required for full-shear-connection. It can be seen that the transverse shear strength is a maximum at $\eta=0$ when the plate is in pure flexure, and that this maximum strength of the transverse shear connection, $2V_{sh}=30$ kN, is only 6% of that required for longitudinal full-shear-connection, $H_{fsc,fi}=543$ kN. The total required strength of shear connection for both longitudinal and transverse shear is $P=H+2V$ and is plotted in Fig. 4(c) where it can be seen that the effect of the transverse forces is quite minimal in this shallow plated beam.

The analyses of the deep plated beams C11 and C12 in the companion paper are shown in Fig. 6(a).

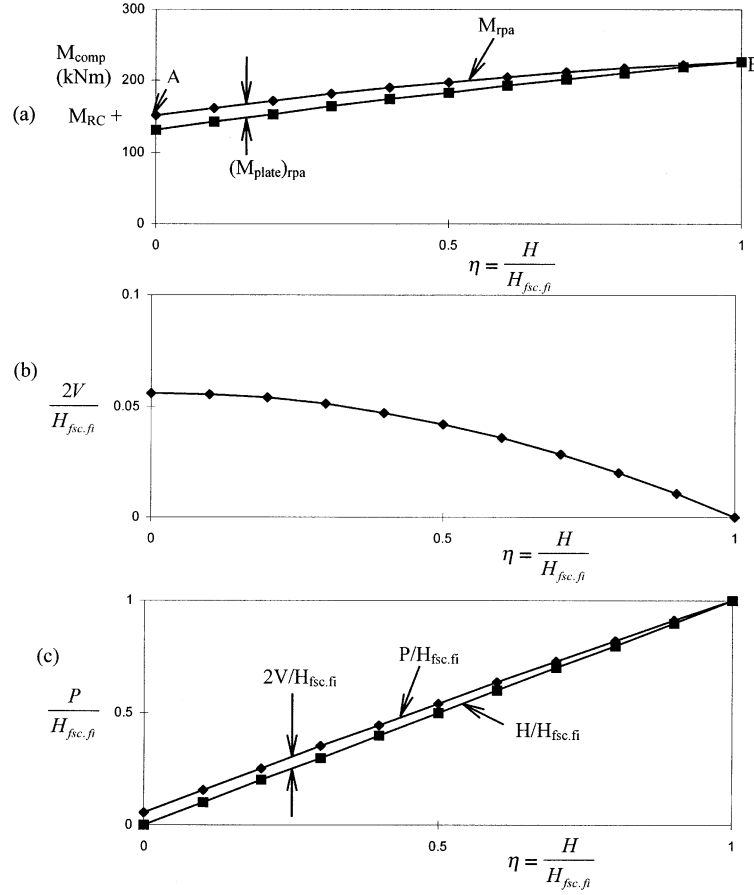
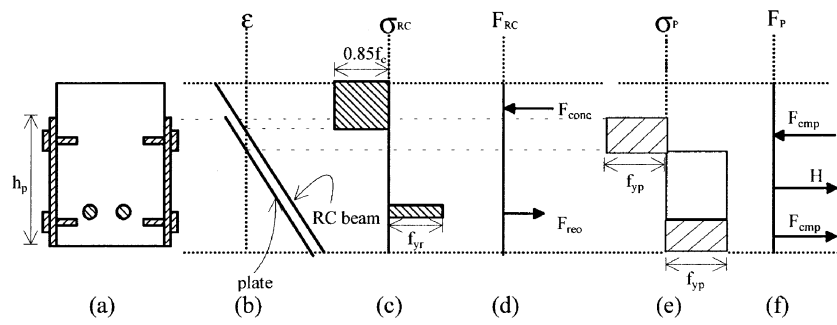


Fig. 4 Shallow plated beams

Fig. 5 Partial-shear-connection analysis for M_{plate}

At point A, $M_{comp} = 218$ kNm which is the sum of the flexural capacity of the reinforced concrete beam of 131 kNm and the flexural capacity of the plate of 87 kNm. At point B, $M_{comp} = 258$ kNm and $H = 587$ kN. The maximum value of $M_{plate} = 87$ kNm and occurs at $\eta = 0$ where M_{plate} is 34% of the composite full-shear-connection capacity $(M_{comp})_{fsc}$ and only reduces to $M_{plate} = 70$ kNm at $\eta = 1$ which is 27% of the maximum flexural capacity. Hence the transverse shear forces remain relatively

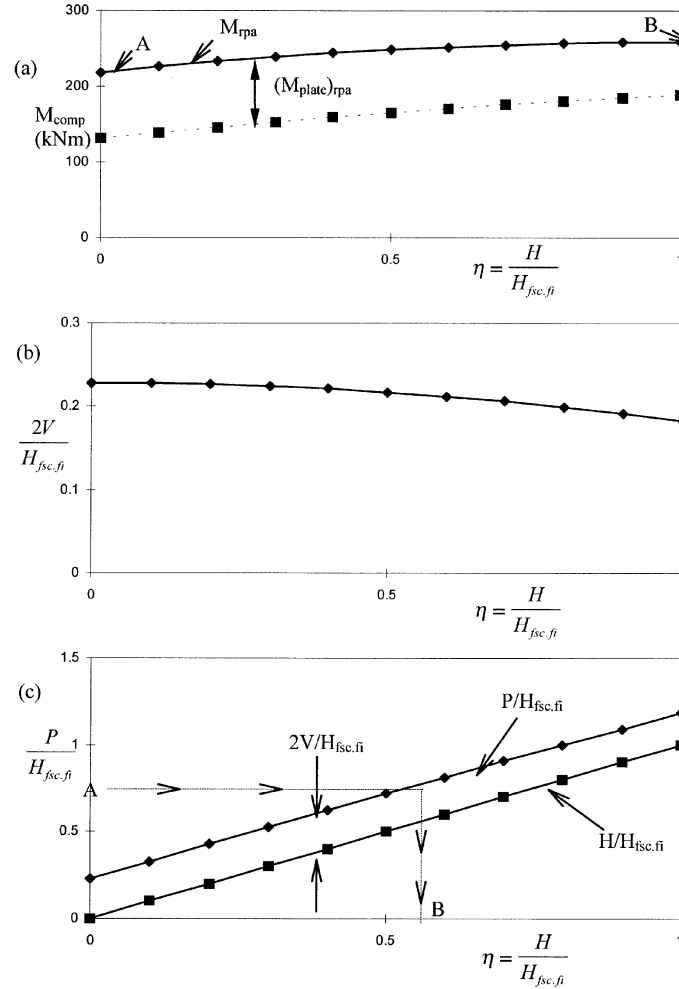


Fig. 6 Deep plated beam

high as shown in Fig. 6(b) where the transverse shear force varies from 23% of $H_{fsc.fi}$ at $\eta=0$ to 18% at $\eta=1$. This is further illustrated in Fig. 6(c) where the total strength of shear connectors required P is substantially more than that required for longitudinal equilibrium H as required in standard rigid-plastic-analysis procedures.

3.2. Mixed analysis

The maximum transverse force in the plate occurs when there is full transverse interaction, that is there is no vertical slip between the plate and the reinforced concrete beam (Oehlers, Nguyen, Ahmed and Bradford 1997). Full transverse interaction also implies that the curvature in the concrete element is the same as that in the plate element, so that $M_{RC} = M_{plate}(EI)_{RC}/(EI)_p$. Substituting this moment into Eq. (1), which was derived from the mixed analysis depicted in Fig. 2, gives

$$(M_{plate})_{mix} = \frac{M - Hh_{cnt}}{\left(1 + \frac{(EI)_{RC}}{(EI)_p}\right)} \quad (8)$$

The moment in the plate, therefore, depends on the applied moment at the section M and the strength of the shear connection H . We can compare this analysis to the moment in the plate from a rigid-plastic analysis at specific degrees of shear connection η^* where the longitudinal shear strength is H_{η^*} , by substituting H_{η^*} for H and $(M_{comp})_{rpa}$ at η^* for M in Eq. (8) which gives

$$(M_{plate})_{mix} = \frac{(M_{comp})_{rpa} - H_{\eta^*}h_{cnt}}{\left(1 + \frac{(EI)_{RC}}{(EI)_p}\right)} \quad (9)$$

Furthermore from Eq. (7), substituting $0.7L_{ss}V$ for M_{plate} gives the transverse strength of shear connection required per shear span, $2V$, as

$$2V = \frac{(M_{comp})_{rpa} - H_{\eta^*}h_{cnt}}{0.35L_{ss}\left(1 + \frac{(EI)_{RC}}{(EI)_p}\right)} \quad (10)$$

The variation of the transverse strength with the degree of shear connection for the beams tested in the companion paper are shown in Fig. 7. In order to produce a conservative design, the flexural rigidity of the cracked reinforced concrete section was used for $(EI)_{RC}$. It can be seen in Fig. 7 that the transverse force for the shallow plated beams is only about 2% of the longitudinal strength required for full-shear-connection. In contrast, the transverse strength required for the deep plated beams is about 15%. This is because, for the shallow plated beams the flexural rigidity of the cracked reinforced concrete section was 22 times the flexural rigidity of the side plates, so that from Eq. (8) it can be seen that the moment in the plate will be very small. However, for the deep plated beams the factor reduced to 3 so that the plates attract a substantial portion of the applied moment. It can also be seen in Fig. 7 that the transverse force is almost constant over the full range of the degree of shear connection so that any discrepancies in the choice of M_{comp} or H will lead to

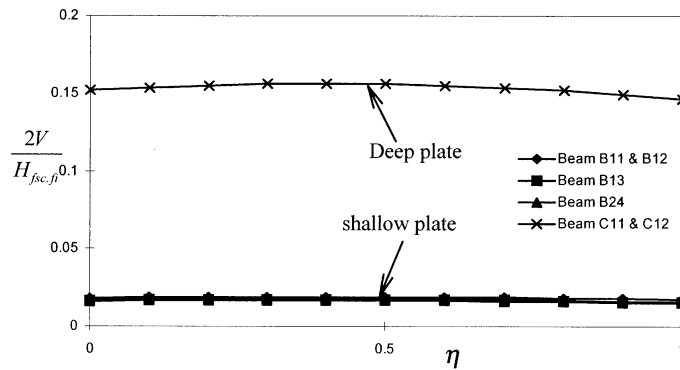


Fig. 7 Transverse forces from mixed analysis

insignificant errors in determining the transverse forces.

4. Rigid plastic bolted-side-plate analysis

The main consideration in the bolted-side-plate analysis that differentiates this technique from standard rigid-plastic analysis procedures is the determination of and the allowance for the plate moment M_{plate} . In order to provide a conservative design, the larger of $(M_{plate})_{mix}$ and $(M_{plate})_{rpa}$ should be used in the bolted-side-plate analysis.

A comparison is made in Fig. 8 between $(M_{plate})_{mix}$ and $(M_{plate})_{rpa}$ for the beams tested in the companion paper. For the deep plated beams, $(M_{plate})_{rpa}$ ranges from 87 kNm at $\eta=0$ to 70 kNm at $\eta=1$, and $(M_{plate})_{mix}$ varies from 58 kNm at $\eta=0$, 59 kNm at $\eta=0.4$ and 56 kNm at $\eta=1$. Therefore, $(M_{plate})_{rpa}$ governs at all degrees of shear connection. In the shallow plated beams, $(M_{plate})_{rpa}$ ranges from 20 kNm at $\eta=0$ to zero at $\eta=1$, whereas $(M_{plate})_{mix}$ remains fairly constant at 7 kNm and, hence, $(M_{plate})_{mix}$ governs at high degrees of shear connection.

4.1. Full shear connection analysis

A full shear connection rigid-plastic analysis is illustrated in Fig. 9. As shown in the companion

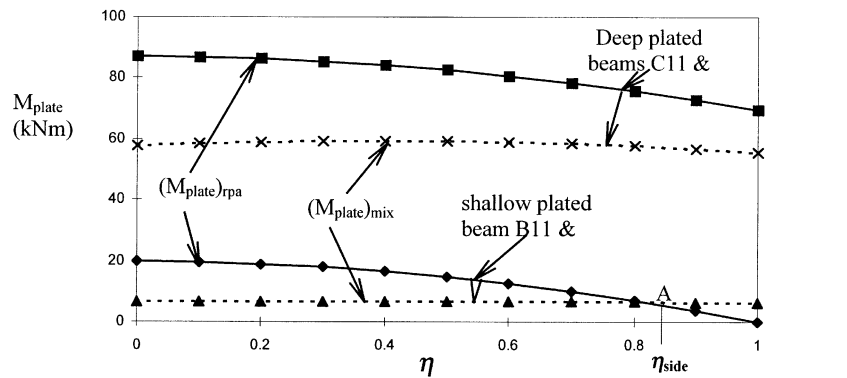


Fig. 8 Moment in plate M_{plate}

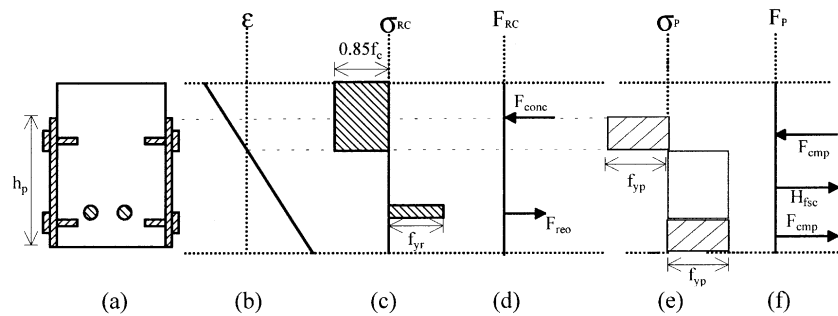


Fig. 9 Full-shear-connection analysis

paper, the best estimate for the flexural capacity and the bond forces occurs when $\gamma=1$ which has been used in this analysis. The strain profiles are coincident as shown in Fig. 9(b) and are moved together vertically until the stress distributions in the reinforced-concrete beam and in the plate in Figs. 9(c) and (e) produce longitudinal forces as in Figs. 9(d) and (f) that have an overall zero resultant. Moments of the forces in Figs. 9(d) and (f) then gives the moment capacity with full shear connection $(M_{comp})_{fsc}$. The stress distribution in the plate in Fig. 9(e) can be broken into the segments shown where F_{cmp} in Fig. 9(f) is the compressive force in the plate which is in equilibrium with a tensile component of the same magnitude as shown. The couple of the forces F_{cmp} is $(M_{plate})_{rpa}$ and the remaining force in the plate H_{fsc} is the strength of the shear connection required for full-shear-connection.

The moment in the plate from the mixed analyses $(M_{plate})_{mix}$ can now be determined from Eq. (9) using $(M_{comp})_{fsc}$ and H_{fsc} derived in the previous paragraph and using the flexural rigidity of the cracked reinforced concrete element for $(EI)_{RC}$ and the remaining elastic properties $(EI)_p$ and h_{cnt} .

When $(M_{plate})_{rpa} > (M_{plate})_{mix}$ then $(M_{plate})_{rpa}$ controls design in which case the flexural capacity of the composite section is $(M_{comp})_{fsc}$. Furthermore as $(M_{plate})_{rpa} = 0.7L_{ss}V$, the strength of the shear connection required in a shear span $2V$ is given by

$$2V = \frac{M_{plate}}{0.35L_{ss}} \quad (11)$$

Therefore, the total strength of shear connection required in the shear span for full-shear-connection is $P = H_{fsc} + 2V$.

4.2. Partial shear connection analysis

A partial-shear-connection analysis has already been illustrated in Fig. 5 where the strain profiles are moved individually until each element is in equilibrium with the longitudinal strength of the shear connection H_{psc} . From this, we can determine the partial-shear-connection moment capacity $(M_{comp})_{psc}$ and the moment in the plate $(M_{plate})_{rpa}$ which is the couple induced by the forces F_{cmp} in Fig. 5(f). The elastic plate moment $(M_{plate})_{mix}$ can be determined from Eq. (9) using H_{psc} and $(M_{comp})_{psc}$. When $(M_{plate})_{rpa} > (M_{plate})_{mix}$ then $(M_{plate})_{rpa}$ controls design and $(M_{plate})_{rpa}$ can be used in Eq. (11) to determine the strength of the transverse shear connectors, so that the total strength of shear connection required in the shear span for partial shear connection is $P = H_{psc} + 2V$.

4.3. Plate moment $(M_{plate})_{mix}$

When $(M_{plate})_{mix} > (M_{plate})_{rpa}$, then $(M_{plate})_{mix}$ controls design, in which case the steps in the analysis are shown in Fig. 10. Fig. 10(A) shows a shear span of a composite plated beam. The plate element is shown by itself in Fig. 10(B) where it can be seen that the shear connectors apply the forces V and H to the plate such that the plate at the section considered is subjected to $(M_{plate})_{mix} = VL_t$ and H as shown in column (a), which induce the stress distributions in column (b). The compressive stresses have a force F_{cmp} in (c) which has a tensile equivalent as shown, and by equating this couple to $(M_{plate})_{mix}$ then F_{cmp} can be determined and, hence, the remaining force in the plate H_{mix} which is the longitudinal strength of the shear connection required when $(M_{plate})_{mix}$ acts. The transverse force can be determined from Eq. (11).

Having determined H_{mix} , we can now consider the reinforced-concrete element by itself as in

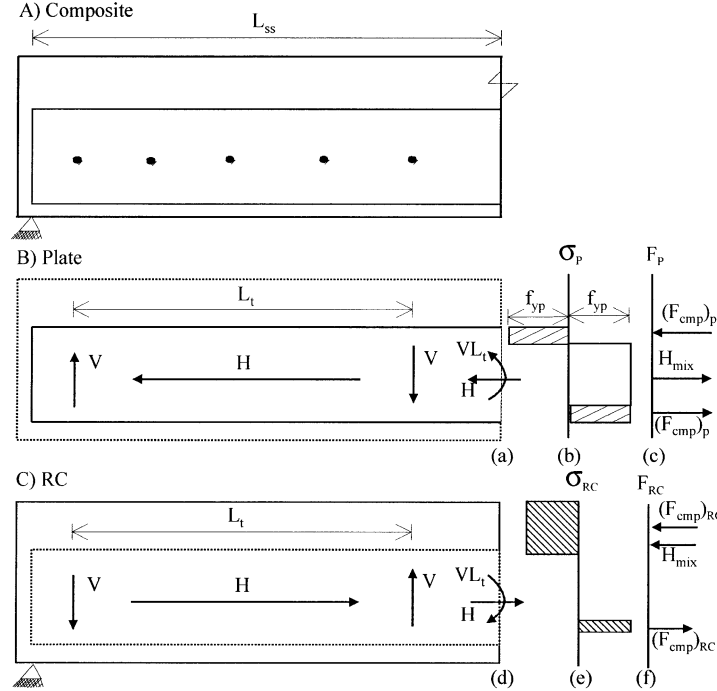


Fig. 10 Full-shear-connection analysis with $(M_{plate})_{mix}$

Fig. 10(C). The shear connector forces have an equal magnitude but opposite direction to those in the plate so that the sum of these stress resultants in columns (a) and (d) is zero. It is now a simple rigid-plastic analysis procedure to determine the stress distribution in (e) when the resultant force in the beam in (f) is H_{mix} , after which the moment capacity of the beam $(M_{comp})_{side}$ can be derived by taking moments of the forces in columns (c) and (f). It can, therefore, be seen that for a specific value of $(M_{plate})_{mix}$, which has been shown to have only a small variation with the degree of shear connection, $(M_{comp})_{mix}$ is fixed. Therefore, H_{mix} is also fixed, which will be referred to as the degree of shear connection $\eta_{side} = H_{mix}/H_{fsc}$. The degree of shear connection η_{side} is shown as point A in Fig. 8 for the shallow plated beams in the companion paper. It is the transition point between $(M_{plate})_{rpa}$ and $(M_{plate})_{mix}$. It is also the greatest degree of shear connection that a plated beam can have when $(M_{plate})_{mix}$ controls the analysis. For example, beam B11 in the companion paper had a degree of shear connection of $\eta = 1.75$ but this beam will behave as a beam with $\eta = \eta_{side} = 0.83$ in Fig. 8.

It is worth noting that in the deep plated beams in Fig. 8, $(M_{plate})_{rpa}$ is always greater than $(M_{plate})_{mix}$ and, hence, $(M_{plate})_{rpa}$ always controls the analysis. Furthermore from Fig. 6(b), the transverse forces $2V$ in the deep plated beam are large so that had the connectors not been supplied to transmit the transverse forces, then the beam would be significantly weaker than expected. In contrast, for the shallow plated beams in Fig. 8, $(M_{plate})_{mix}$ is usually less than $(M_{plate})_{rpa}$ and the transverse forces shown in Fig. 4(b) are insignificant and can be ignored in practice. However, if these shallow plated beams had full-shear-connection then they would be weaker than expected as they now act as if they had partial-shear-connection of η_{side} .

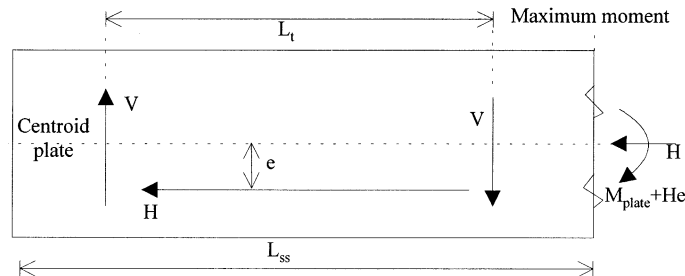


Fig. 11 Eccentricity of connector force

4.4. Eccentricity of H

To complete the method of analysis, let us now consider a plate that is subjected to a longitudinal shear force at an eccentricity e below the centroid of the plate as shown in Fig. 11; this can occur due to transverse interaction as explained in the companion paper. Comparing the stress resultants in this figure with those in Fig. 10(B), it can be seen that the plate has to resist an additional moment He which will reduce the flexural strength of the composite section. In contrast, it is worth noting that deliberately distributing the shear connectors so that their resultant force lies above the centroid of the plate will increase the flexural capacity.

5. Allowance for h_{na} and $\Delta\kappa$

The results of the beam tests in the companion paper were analysed using the rigid-plastic bolted-side-plated analysis in the previous section, which allows for the effects of the transverse force, in order to determine the reduction in strength due to the neutral axis separation h_{na} and difference in curvature $\Delta\kappa$ described in the companion paper. As an example of the analysis procedure, Fig. 6(c) was first formed for the deep plated beams. As the total strength of the shear connection in a shear span P of the deep plated beam is known such as at point A, the degree of longitudinal shear connection at point B can be determined directly by following the arrowed line. In these analyses, it was assumed that $\gamma=1$ in contrast to the analyses presented in the companion paper where γ was assumed to be slightly less.

The results of the analysis described in the previous paragraph are listed in Table 1. The strengths of the shear connectors in a shear span in column 2 range from 22% to 175% of the strengths of the plates in column 3. From a side-plated rigid-plastic analysis: the strengths required for a full-interaction full-shear-connection are listed in column (4); from which the degree of shear connection provided can be determined as in column (5) which ranges from 43% to 175%. From a bolted-side-plated-beam analysis: the moment in the plate that controls the design is listed in column 6; the degree of shear connection in column 7 now ranges from 22% to 83%; the longitudinal strength of the shear connection is in column 8; the transverse strength in column 9 which ranges from 2% to 105% of the longitudinal strength; and the total strength in column 10. The subscript 'side' has been used in columns 7 to 10 to refer to this new rigid-plastic analysis approach for bolted-side-plated beams.

The experimentally determined increase in strength due to plating, as a proportion of the original strength of the unplated beam, is listed in column 12, and the theoretical increase in strength from a

Table 1 Analysis of beam tests

Beam # (1)	P_{exp} kN (2)	$A_{p/yp}$ kN (3)	$(P_{rpa})_{fsc}$ kN (4)	η_{rpa} (5)	M_{plate} (6)	η_{side} (7)	H_{side} kN (8)	$2V_{side}$ kN (9)	P_{side} kN (10)
B11	950	543	543	1.75	mix	0.83	449	10	459
B12	259	543	543	0.48	rpa	0.43	234	25	258
B13	259	599	599	0.43	rpa	0.38	230	29	259
B24	493	543	543	0.90	mix	0.83	450	10	460
C11	432	1199	587	0.74	rpa	0.52	305	127	432
C12	259	1199	587	0.44	rpa	0.22	126	133	259

Beam # (11)	ΔM_{exp} (12)	ΔM_{side} (13)	error % (14)	Sequence of failure (15)
B11	0.564	0.663	-14.9	concrete crushed
B12	0.410	0.464	-11.6	concrete crushed; support bolt fractured
B13	0.471	0.478	-1.5	concrete crushed; mid-span bolt fractured
B24	0.600	0.618	-2.9	concrete crushed
C11	0.700	0.891	-21.4	plate buckled; concrete crushed
C12	0.700	0.776	-9.7	concrete crushed; support bolt fractured

bolted-side-plated analysis in column 13. It can be seen that the experimental increases in strength are consistently lower than the theoretical strengths and this consistent reduction can be considered due to the h_{na} and $\Delta\kappa$ effects. The percentage error is listed in column 14. If we ignore the result for beam C11 which failed prematurely through buckling as shown in column 15, then the % errors range from 2% to 15% with a mean of 8%. It needs to be remembered that this is the error in the increase in strength and that the error as a proportion of the composite strength of the side plated reinforced concrete beam ranges from 1% to 10%. It is, therefore, suggested that for a lower confidence limit, the increase in the theoretical strength should be reduced by 15% to allow for the h_{na} and $\Delta\kappa$ effects, until more tests become available and until the present research (Oehlers, Nguyen, Ahmed and Bradford 1997) is extended to allow for non-linearity.

6. Application

Plates are bolted to the continuous reinforced concrete T-beam in Fig. 12 in both the negative and positive regions as shown. The reinforced concrete T-beam has a flange width of 2m, web width of 800 mm, slab depth of 250 mm and web depth of 550 mm. In the negative region, the area of the tension reinforcing bars is 20,000 mm² at 50 mm from the top surface, the plates are 550 mm deep and 10 mm thick, the plate extends 2.4 m from the support and all of the plate is within the negative region. In the positive region, the area of the tension reinforcing bars is 10,000 mm² at 50 mm from the soffit, the plates are 550 mm deep and 5 mm thick, the plate extends 4 m from mid-span and all of the plate is within the positive region. The material properties consist of, $f_c = 30$ MPa, $E_{conc} = 30,000$ MPa; $f_{yr} = 400$ MPa, $f_{yp} = 350$ MPa, and $E_{steel} = 210,000$ MPa.

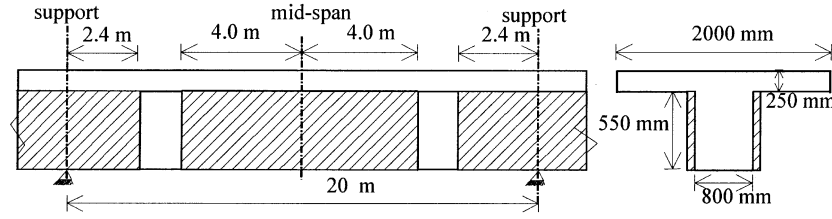


Fig. 12 Plated internal bay

6.1. Case 1: Positive region with full-shear-connection

The analyses showed that $(M_{plate})_{rpa} = 0$ so that $(M_{plate})_{mix}$ controls the design. The results of the analyses gave: $M_{RC} = 2,844$ kNm; $(M_{comp})_{jsc} = 3,667$ kNm; $(EI)_{RC}/(EI)_p = 28$; $h_{cni} = 328$ mm; $(M_{plate})_{mix} = 61$ kNm; $H_{jsc} = 1,925$ kN; $2V = 44$ kN; $P = 1969$ kN; $\eta_{side} = 0.88$; $(M_{comp})_{mix} = 3546$ kNm; and a design capacity $(M_{comp})_{design} = 3441$ kNm which allows for the 15% reduction due to the h_{na} and $\Delta\kappa$ effects.

From a rigid plastic analysis, the addition of the side plates would increase the strength by 823 kNm which can be considered as an upper bound to the increase. However, the transverse forces will reduce this increase to 702 kNm and the effect of h_{na} and $\Delta\kappa$ will reduce it further to 597 kNm. Hence, the composite plated beam has a strength of 3441 kNm which is 6% smaller than that predicted by a side-plated rigid plastic analyses.

The following points are also worth noting: the additional strength of shear connectors required to resist the transverse forces is insignificant at only 2% of the strength required for the longitudinal shear and; the plate transfers a vertical shear force of $V_{sh} = 22$ kN which in effect is the increase in the vertical shear strength of the beam which in this case is insignificant; and as all of the plate is primarily in the tension region, the positive region of the beam will behave in a brittle fashion with limited ability to redistribute moment if required.

6.2. Case 2: Hogging region with full shear connection

The analyses showed that $(M_{plate})_{rpa}$ controls the design. The results of the analyses gave: $M_{RC} = 4,432$ kNm; $(M_{plate})_{rpa} = 418$ kNm; $(M_{comp})_{jsc} = 5,023$ kNm; $(EI)_{RC}/(EI)_p = 17$; $h_{cni} = 91$ mm; $(M_{plate})_{mix} = 268$ kNm; $H_{jsc} = 966$ kN; $2V = 498$ kN; $P = 1464$ kN; and $(M_{comp})_{design} = 4934$ kNm.

From a rigid plastic analysis, side plating would increase the strength by 591 kNm which is reduced by the effect of h_{na} and $\Delta\kappa$ to 502 kNm. Hence, the composite plated beam has a strength which is 2% smaller than that predicted by a side-plated rigid-plastic analyses. The transverse forces are significant in this case being 52% of the longitudinal forces and the additional shear connectors required to transfer the vertical shear significantly increases the shear strength of the beam by 249 kN. As the neutral axis lies within the plate, the composite plated beam will behave in a ductile fashion allowing moment to be redistributed from the hogging region to the sagging region.

6.3. Case 3: Sagging region with partial shear connection

It is assumed in this analysis that $\eta = 0.6$ which is less than $\eta_{side} = 0.88$ in Case 1 so that $(M_{plate})_{rpa}$ will control the design. The results of the analyses gave: $M_{RC} = 2,844$ kNm; $(M_{comp})_{psc} = 3,518$ kNm; $H_{psc} = 1,155$ kN; $2V = 121$ kN; $P = 1276$ kN; and $(M_{comp})_{design} = 3417$ kNm. The composite plated

beam has a strength which is 3% smaller than that predicted by a side-plated rigid plastic analyses.

7. Conclusions

An analysis technique has been developed for determining the increase in both the flexural strength and in the shear strength of bolting plates to the sides of reinforced concrete beams. The technique allows for any number of connectors and for the detrimental effects of both vertical and longitudinal slip. It is shown that side plated beams may need substantially more connectors than standard rigid plastic analysis techniques would suggest, but these additional connectors can also substantially increase the vertical shear capacity of the beam. The technique can be applied to both the positive and negative regions of continuous reinforced concrete beams.

Acknowledgements

This work forms part of an ongoing research project between the Universities of New South Wales and Adelaide that is funded by a Large Australian Research Council Grant.

References

- Ahmed, M. (1996), "Strengthening of reinforced concrete beams by bolting steel plates to their sides", Master of Engineering Science Thesis, The University of Adelaide, Australia, October.
- Ahmed, M., Oehlers, D.J. and Bradford, M.A. (2000), "Retrofitting reinforced concrete beams by bolting steel plates to their sides. Part 1: Behaviour and experimental work", *Structural Engineering and Mechanics, Int'l Journal*, **10**(3).
- Oehlers, D.J. and Sved, G. (1995), "Flexural strength of composite beams with limited slip capacity shear connectors", *Journal of Structural Engineering, ASCE*, **121**(6), Jun., 932-938.
- Oehlers, D.J., Nguyen, N.T., Ahmed, M. and Bradford, M.A. (1997), "Transverse and longitudinal partial interaction in composite bolted side-plated reinforced-concrete beams", *Structural Engineering and Mechanics, An Int'l Journal*, **5**(5), Sept., 553-564.
- Smith, S.T., Bradford, M.A. and Oehlers, D.J. (1999a), "Local buckling of side-plated reinforced concrete beams. Part 1: Theoretical study", *ASCE, Journal of Structural Engineering*, June 622-634.
- Smith, S.T., Bradford, M.A. and Oehlers, D.J. (1997b), "Local buckling side-plated reinforced concrete beams. Part 2: Experimental study", *ASCE, Journal of Structural Engineering*, June 635-643.

Notation

E	= Young's modulus
EI	= flexural rigidity
e	= eccentricity of longitudinal or horizontal shear force
F	= force; force profile
f_c	= cylinder strength of concrete
f_{yp}	= yield strength of plate
f_{yr}	= yield strength of reinforcing bar
H	= strength of shear connection required to resist longitudinal or horizontal shear forces; horizontal force

h_{ent}	= distance between centroids of plate and RC element
h_{na}	= neutral axis separation
L	= half span of beam
L_{ss}	= length of plate shear span
L_t	= lever arm of resultant transverse shear forces
M	= moment; moment capacity
P	= strength of shear connection in a shear span
q	= shear flow strength
s_v	= transverse or vertical slip
V	= transverse force
x	= distance along shear span from support
y	= deflection
Δy	= change in deflection
$\Delta \kappa$	= difference in curvature between plate and RC elements
ΔM	= increase in flexural capacity due to plating
ε	= strain; strain profile
γ	= neutral axis parameter
η	= degree of shear connection
κ	= curvature
σ	= stress profile

frequently used suffices:

<i>conc</i>	= concrete
<i>cmp</i>	= compressive
<i>comp</i>	= composite beam; composite
<i>design</i>	= allows for 15% reduction in the increase in strength
<i>exp</i>	= experimentally determined
<i>fi</i>	= full interaction
<i>free</i>	= plate free of support
<i>fsc</i>	= full shear connection
<i>mix</i>	= mixed analysis
<i>p</i>	= plate
<i>psc</i>	= partial shear connection
<i>rpa</i>	= standard rigid plastic analysis
<i>RC</i>	= reinforced concrete
<i>reo</i>	= reinforcing bars
<i>rest</i>	= plate resting on support
<i>side</i>	= derived from new bolted-side-plated analysis technique